



## Novel 3D printing-based probe for impedance spectroscopic examination of oral mucosa: design and preliminary testing with phantom models

Shekh Emran , Kimmo Laitinen , Reijo Lappalainen & Sami Myllymaa

To cite this article: Shekh Emran , Kimmo Laitinen , Reijo Lappalainen & Sami Myllymaa (2020): Novel 3D printing-based probe for impedance spectroscopic examination of oral mucosa: design and preliminary testing with phantom models, Journal of Medical Engineering & Technology, DOI: [10.1080/03091902.2020.1831633](https://doi.org/10.1080/03091902.2020.1831633)

To link to this article: <https://doi.org/10.1080/03091902.2020.1831633>



© 2020 The Author(s). Published by Informa UK Limited, trading as Taylor & Francis Group.



Published online: 02 Nov 2020.



Submit your article to this journal [↗](#)



Article views: 144



View related articles [↗](#)



View Crossmark data [↗](#)

# Novel 3D printing-based probe for impedance spectroscopic examination of oral mucosa: design and preliminary testing with phantom models

Shekh Emran<sup>a,b</sup> , Kimmo Laitinen<sup>a</sup>, Reijo Lappalainen<sup>a,b</sup> and Sami Myllymaa<sup>a,b</sup> 

<sup>a</sup>Department of Applied Physics, University of Eastern Finland, Kuopio, Finland; <sup>b</sup>SIB Labs, University of Eastern Finland, Kuopio, Finland

## ABSTRACT

The diagnosis of oral potentially malignant disorders currently relies on histopathological examination of surgically removed biopsies causing pain and discomfort for the patient. We hypothesise that non-invasive bioimpedance spectroscopy (BIS) method would overcome these problems and could make possible regular screening of at-risk patients. Previously several hand-made probes have been introduced in such BIS studies. However, for the first time, we aimed to design a 3D printed probe and test it with model samples (saline solutions, cucumber and porcine tongue). We found that it is extremely crucial to select proper printable materials and optimise electrode geometries to avoid electrochemical corrosion problems, short-circuiting and other signal instabilities related to miniaturised probe. However, our final prototype constructed with four high purity silver made electrodes showed a good linearity ( $R^2 = 0.999$ ) in diluted saline solution measurements over a wide conductivity range (0.25–8 mS/cm), which covers well the range of values for the different biological tissues. Moreover, our data show that high reproducibility of the manufacturing and measurement is one important merit in the present 3D printed probe. However, further studies are needed to clarify the importance of fixed pressure especially when the tetrapolar 3D printed probe is used as a hand-held apparatus.

## ARTICLE HISTORY

Received 14 August 2020  
Revised 21 September 2020  
Accepted 29 September 2020

## KEYWORDS

Bioimpedance spectroscopy; 3D printed probe; concentric ring probe; oral mucosal diseases; oral cancer

## 1. Introduction

Oral cancer is one of the most common cancers with approximately 270,000 new cases and 120,500 deaths occurring annually [1]. Oral cancer has one of the highest 5-year mortality rates (50%) of all cancers, probably because many oral malignancies are not diagnosed until the late stages of the disease [2]. The prognosis depends to a great extent on the stage of diagnosis and thus it would be very beneficial that the disease could be screened and detected at its early or precancerous stages [3,4].

Most oral malignancies are oral squamous cell carcinomas (OSCCs). OSCCs are thought to progress from potentially malignant lesions, beginning as hyperplastic tissue and developing into an invasive squamous cell carcinoma [5]. Oral potentially malignant disorders (OPMDs) refer to all epithelial lesions and conditions with an increased risk for malignant transformation [6]. OPMDs include several different entities such as oral leukoplakia, oral erythroplakia, oral sub mucous fibrosis, oral lichen planus and oral candidiasis. Some of OPMDs are often invisible to the naked eye and can have an

appearance, which is indistinguishable from a benign lesion [7].

The diagnosis of oral cancer and OPMDs currently relies on a histological and immunohistological analysis of surgically removed biopsies. The procedure involved in gathering the surgical biopsy is invasive, causing pain and discomfort for the patient. It is also expensive and time-consuming [8]. A non-invasive method for diagnosing OPMDs would overcome these problems and would allow affordable regular chairside screening (e.g., at dental clinics) at risk patients and could make possible regular screening of at-risk patients. This would be particularly beneficial in the treatment of oral cancer where the low survival rates are attributable to late diagnosis [9]. To prevent malignant transformation of these oral premalignant lesions, new non-invasive point-of-care detection techniques are urgently needed to address this global health problem.

Bioimpedance is the measure of the opposition that a circuit presents to a current when a voltage is applied. Using bioimpedance spectroscopy (BIS) technique, the impedance of biological tissues can be

**CONTACT** Sami Myllymaa  sami.myllymaa@uef.fi  SIB Labs, University of Eastern Finland, Kuopio, Finland

© 2020 The Author(s). Published by Informa UK Limited, trading as Taylor & Francis Group.

This is an Open Access article distributed under the terms of the Creative Commons Attribution-NonCommercial-NoDerivatives License (<http://creativecommons.org/licenses/by-nc-nd/4.0/>), which permits non-commercial re-use, distribution, and reproduction in any medium, provided the original work is properly cited, and is not altered, transformed, or built upon in any way.

determined over a wide frequency range [10]. Biological tissues (cells, intra- and extracellular space, matrices) have resistive and capacitive elements that result in complex impedance values when applying low-intensity electrical current to the tissues. Measuring the impedance parameters of cells across a range of frequencies will produce an impedance spectrum that is characteristic for the biological tissue and reflects the chemical and structural alterations in the tissue. Overall, there is abundant research and scientific articles related to use of impedance-based methods in various biomedical applications such as in skin cancer diagnostics [11–15]. However, the BIS studies concerning the evaluation of oral mucosa condition and assessment of oral mucosal diseases are rare [3,9,16].

When considering *in vivo* BIS measurements inside the oral cavity, more standardised measurements are needed [17], and a new sensor design is required [9]. It should be cheap to fabricate with mass production techniques, patient-safe and single-use to avoid cross-contamination or need of any sterilisation steps. 3D printing may offer such technological opportunities, and this study is focussed on clarifying the real potential of 3D printing technology in constructing BIS probe or its components for oral mucosa examination. There are several measurement methods (two-electrode, three-electrode, four-electrode, etc.) available for performing electrochemical experiments [18]. Two-electrode is a convenient method to obtain basic information about the electrical characteristics of a given test sample whereas a major drawback is that the contact impedances of two electrodes can influence the obtained results [19]. However, in a four-electrode method, separate electrode pairs are used as current and voltage electrodes eliminating the contact impedance from the measurement. Thus, using four-electrode method will increase the measurement stability (e.g., reduce the importance of fixed pressure) and minimise the effect of electrode geometry on BIS measurements [9]. In this study, we aimed to design a 3D printed probe with four high purity silver electrodes configuration and test it with various phantom materials (biological and non-biological) and porcine tongue samples. Furthermore, we wanted to compare the results of four electrode 3D printed probe with the conventional concentric ring probe (two electrodes).

## 2. Materials and methods

### 2.1. Design of the 3D printed probe

A novel 3D printed probe consisting of four high purity silver electrodes was designed for oral tissue

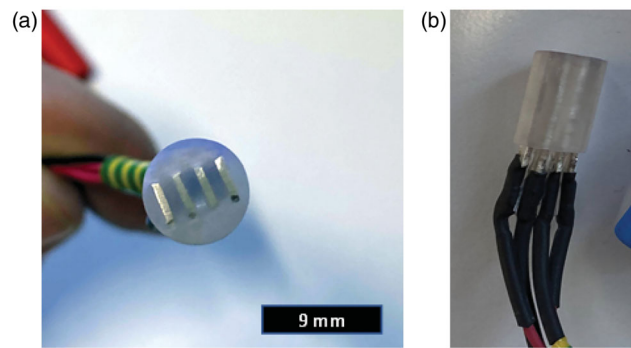


**Figure 1.** (a) The final version of the bioimpedance spectroscopy (BIS) probe head with four high-purity silver electrodes. The electrode contact areas are 4 mm × 0.6 mm. (b) The good mechanical and electrical stability of the BIS probe is assured with a 3D printed plastic frame that ensures 1 mm insulation layer between adjacent electrodes. The wires terminated to 4 mm banana sockets are directly soldered to the silver electrode plates.

biopsy measurements. Before constructing the final version of the probe (Figure 1), several prototype versions were designed and tested in BIS measurements. We learned that it was extremely crucial to select proper printable insulator materials and optimise electrode geometries and materials to avoid electrochemical corrosion problems, short-circuiting and other signal instabilities related to miniaturised probe with short dimensions (Table 1).

As a result of prototyping, a fully functional 3D printed probe for BIS measurements was realised (prototype 7, Table 1) and its reliability, repeatability and accuracy were confirmed with versatile test measurements. Thus, after initial study we used the latest version probe for our further measurements.

The final version probe composed of four rectangular shaped high purity silver electrodes (each electrode with 4 mm × 0.6 mm × 11 mm size) inserted in a 3D printed holder block ensuring 1 mm insulation between adjacent electrodes (Figure 1). The probe was designed with Fusion 360 software (Autodesk Inc., San Rafael, CA) and the holder block was printed using a Formlabs Form 2 (Formlabs, Somerville, MA) 3D printer (Figure 2).

This probe, about 9 mm in diameter and about 15 mm in length, can be placed on *ex vivo* tissue sample in a simple mechanical setup to ensure a proper pressure on a biopsy with a diameter of 8 mm. Figure 2 shows a plane top view of the tip of the probe, in which A–D are the electrodes. One pair of electrodes (A–D) was used for current injecting and others (B–C) were used for voltage measurement. The electrodes

**Table 1.** Different steps towards successful probe construction.

Prototype (s)	Electrode materials	Insulating materials	Remarks
Prototype 1	1 mm thick non-passivated stainless steel (AISI316L)	Single material; Formlabs Standard Clear FLGPCL04	Heavily corroded during BIS measurement
Prototype 2	1 mm thick passivated stainless steel (AISI316L)	Single material; Formlabs Standard Clear FLGPCL04	Corroded and inconsistent impedance data found after few minutes
Prototype 3	0.6 mm thick passivated stainless steel (AISI316L)	Multimaterial; Vero PureWhite	Corroded, insulation also showed conductivity, no measurements done
Prototype 4	0.6 mm thick passivated stainless steel (AISI 304)	Single material; Formlabs Standard Clear FLGPCL04	Corroded after five to six minutes
Prototype 5	0.6 mm thick passivated stainless steel (AISI 304)	Teflon insulation (handmade probe)	Corroded after few measurements
Prototype 6	0.6 mm thick tantalum electrodes	Single material; Formlabs Standard Clear FLGPCL04	High impedance values
Prototype 7	0.6 mm thick high purity silver (fine silver 999, Peltolan Spectrolitnappi Ky, Pertunmaa, Finland)	Single material; Formlabs Standard Clear FLGPCL04	Fully functional, present data are based on this prototype

Seven different prototypes were realised.

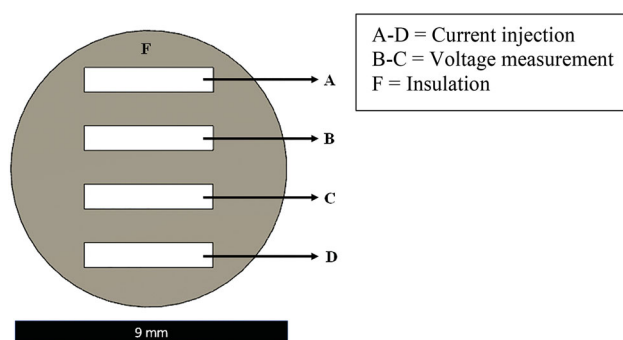


**Figure 2.** A cross-sectional layout view of the custom-made bioimpedance probe with four rectangular high purity silver electrodes (A–D) inside the 3D printed insulation block (F).

were soldered to the copper cables terminating to 4 mm banana sockets (Hirschmann Test, SKS Kontakttechnik GmbH, Niederdorf, Germany) through which the probe was connected to an electrical impedance analyser.

## 2.2. Measurement setup

Our novel 3D printed probe with a 200 g loading was placed in a probe stand (Figure 3). The measurement cables were connected to a Solartron 1260 impedance/gain-phase analyser coupled to a Solartron 1287 electrochemical interface (Solartron Analytical, Farnborough, UK). For 3D printed probe, outer terminals (A–D) of the probe are connected through the CE and WE connection cables whereas, inner two (B–C) are connected through the RE1 and RE2 connection cables.

The BIS data were collected and stored using a laptop running Z-plot software (Scribner Associates Inc., Southern Pines, NC). The frequency range for the sinusoidal excitation signal was set between 1 Hz and 3 MHz with an amplitude of 50 mV.

## 2.3. Functionality testing

To test the functionality of the 3D printed probe, different mixtures of saline solutions and biological samples (cucumber and porcine tongue) were used as phantom materials. In the first part of the study, six mixtures of saline solutions were used to verify whether the 3D printed probe can discriminate solutions with different conductivities and to check the linearity of the response. The solutions were prepared by serially diluting a NaCl solution with a conductivity of 16 mS/cm with deionised water (Table 2). The BIS measurements were conducted by immersing the probe into the diluted solutions. For each solution, three repeated BIS measurements ( $n=3$ ) were performed. Admittance (reciprocal of impedance) and its standard deviation were calculated at 377.67 Hz where the response was the most resistive (phase value closest to zero).

After that, two biological samples, i.e., cucumber and pork tongue were measured. A porcine tongue was taken from the freezer and immediately after thawing the samples were excised. BIS measurements were performed immediately after sample preparation. In this part of study, both custom-made concentric probe (Figure 4) and 3D printed probe were used. The BIS data were measured considering three locations for each set of samples (Figure 5) using four-terminal measurements with the 3D printed probe and two-terminal measurements with the concentric ring probe. A fixed load of 200 g was systematically used.

Three BIS scans were conducted, and each measurement took approximately 2 min with a 1-min break before the next scan. To make intra-location variation easier to interpret, relative standard deviations (RSDs; also termed coefficient of variation, CV) were calculated for magnitude data and standard deviations for phase data of repeated measurements.

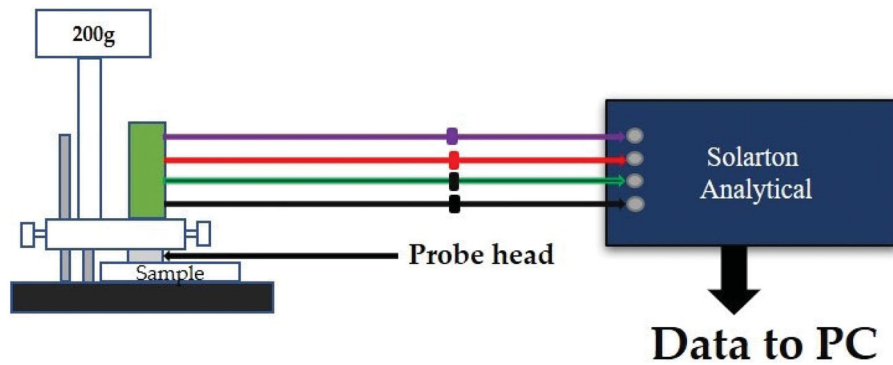


**Figure 3.** Schematic overview of the experimental setup for bioimpedance spectroscopic measurements with 3D printed probe (modified from Emran et al. [9]).

**Table 2.** Mixtures of saline solutions and their nominal conductivities used as test solutions.

Nominal conductivity of test solution (mS/cm)	
Solution 1: mixture of solution 1- & 1-part H <sub>2</sub> O	8 mS/cm
Solution 2: mixture of solution 2- & 1-part H <sub>2</sub> O	4 mS/cm
Solution 3: mixture of solution 3- & 1-part H <sub>2</sub> O	2 mS/cm
Solution 4: mixture of solution 4- & 1-part H <sub>2</sub> O	1 mS/cm
Solution 5: mixture of solution 5- & 1-part H <sub>2</sub> O	0.5 mS/cm
Solution 6: mixture of solution 6- & 1-part H <sub>2</sub> O	0.25 mS/cm

conductivity of test solution (from solution 1 to solution 6). Up to 100 kHz, the phase (theta values) was almost negligible. At a specific examination frequency of 377.67 Hz, the BIS measurements with serially diluted NaCl solutions with a wide conductivity range (0.25–8 mS/cm) showed excellent linearity ( $R^2=0.999$ , Figure 6(b)).

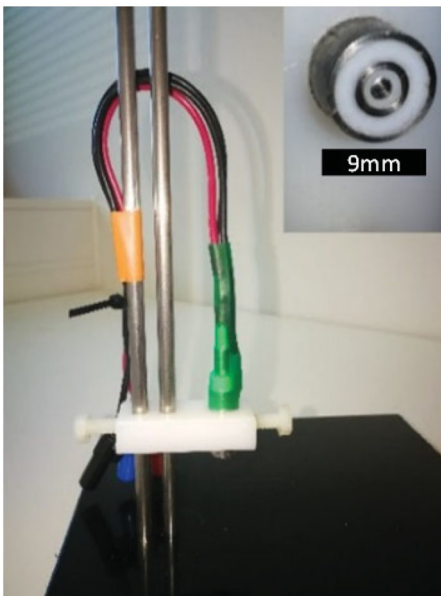


**Figure 4.** A custom-made concentric bioimpedance probe [9] used for comparison. Two terminal measurements were conducted by connecting outer ring and central pin, i.e., both current injection and voltage measurement was performed using the same electrode pair. The probe head is shown in the upper right corner of the picture.

### 3. Results

#### 3.1. Saline solution measurements

Bode plots (Figure 6(a)) for serially diluted NaCl solutions displayed systematically increase impedance magnitude alongside with decreasing nominal

#### 3.2. Cucumber and porcine tongue measurements

Intra-sample variation was tested using cucumber and porcine tongue as biological test model samples. The BIS spectra obtained for three adjacent locations of cucumber sample with a fixed loading weight (200 g) are shown in Figure 7. In the case of 3D printed probe, impedance magnitude values were almost constant up to 1 kHz and beyond that frequency the impedance values lowered. After 1 kHz, there was a rapid drop in phase values, too. The inter-scan variation in each location was low indicating a good repeatability of measurement. The RSDs of impedance magnitude were below 3.5% over the whole frequency range. The STDs of phase were all low (below 0.9°). In case of concentric probe, impedance was more dependent on the excitation frequency; magnitude increased with decreasing frequency and compared to 3D printed probe, phase became more negative at frequencies below 100 Hz. Compared to 3D printed probe, the RSDs of impedance magnitude varied more between the different locations and the highest RSDs were close to 6%. The STDs of phase were constantly low (below 1.5°).

The BIS data obtained from three different locations of porcine tongue sample are shown in Figure 8. In case of 3D printed probe, impedance magnitudes were generally low and highly independent on excitation frequency. Generally, there was a trend towards slightly increased impedance magnitudes from the first scan to the third one. Up to 10 kHz, phase values



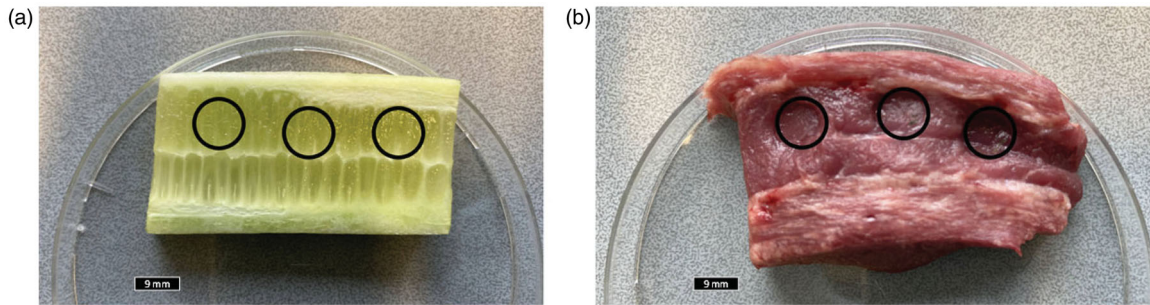


**Figure 5.** Biological samples (5 mm thick slices) used to evaluate the performance of the novel 3D printed probe: (a) cucumber and (b) pork tongue with indicated measurement locations.

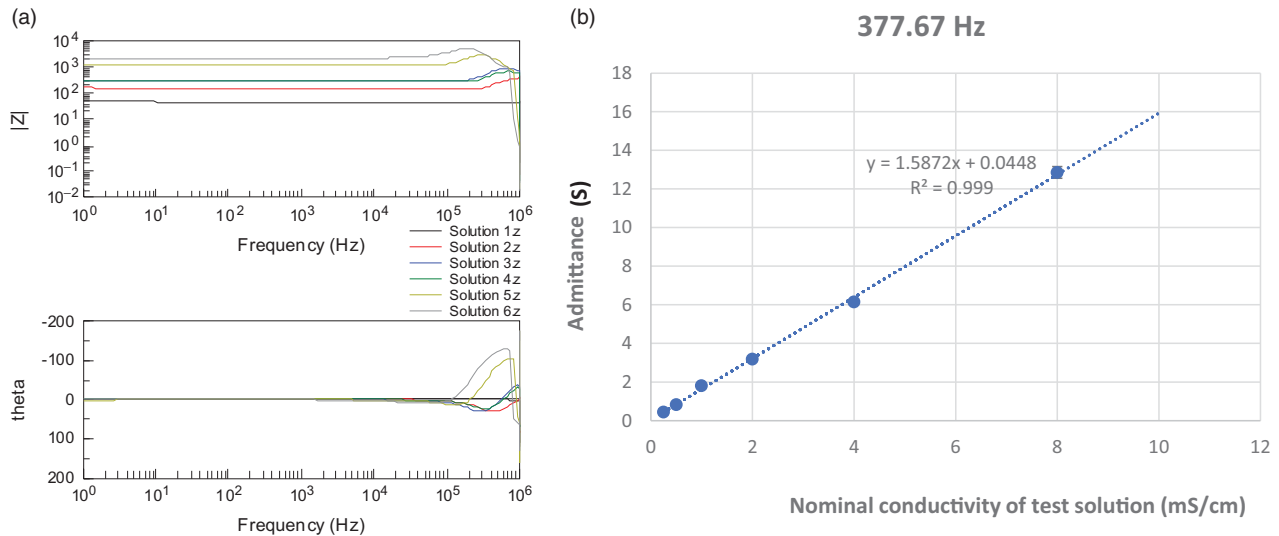


**Figure 6.** (a) Bode plots for all mixtures of NaCl solutions; (b) measured admittance as a function of nominal conductivity of NaCl test solutions shows excellent linearity ( $R^2=0.999$ ).

were almost negligible. The inter-scan variation in each location was low indicating good repeatability of measurement. The RSDs of impedance magnitude varied between 4.7 and 9.1% within the range of 1 Hz to 10 kHz. The STDs of phase were all low ( $0.03\text{--}2.92^\circ$ ). In case of concentric probe, impedance was highly dependent on the excitation frequency, i.e., the impedance magnitude increased, and phase became more negative with decreasing frequency. In contrast to 3D printed probe, there was a trend towards slightly decreased impedance magnitudes from the first scan to the third one. Compared to 3D printed probe, the RSDs of impedance magnitude varied more between the different locations.

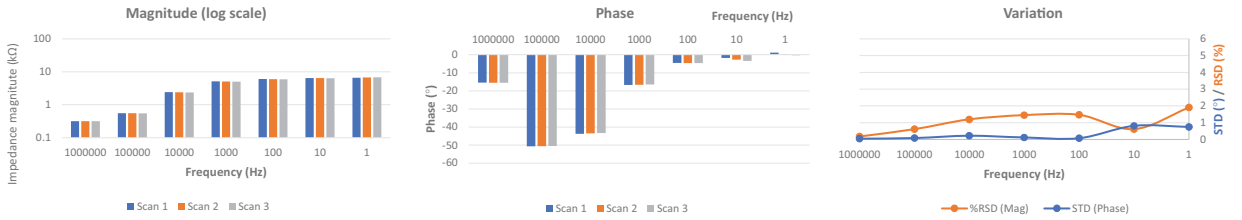
#### 4. Discussion

The main goal of the present study was to design and test a new 3D printed probe for four-terminal BIS measurements. The feasibility testing was conducted with saline solutions and biological test samples. Overall, the obtained BIS results were promising

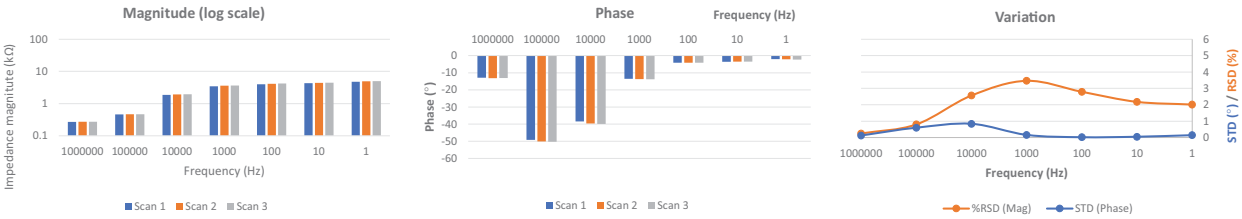
showing that the present tetrapolar probe can reliably characterise the samples having different electrical conductivity properties along with an excellent measurement reproducibility.

Designing a successful 3D printed probe for BIS measurements was a challenging task. Before implementing the successful probe, we constructed several prototype versions considering several factors such as biocompatibility, electrical stability, corrosion and short circuiting (Table 1). We found that choosing proper electrode material is a critical issue as electrode surfaces are easily corroded in such kind of electrolyte/biological tissue measurements. At the beginning of prototyping process, we used different types of stainless steel (SS) as an electrode material. However, most of the stainless-steel electrodes tended to be corroding after few seconds depending on the size of the probe and the applied excitation voltage. Moreover, we constructed a prototype with tantalum (Ta) electrodes in order to solve the corrosion problem [20]. Albeit the corrosion was not issue anymore, impedance magnitude was observed to be too high

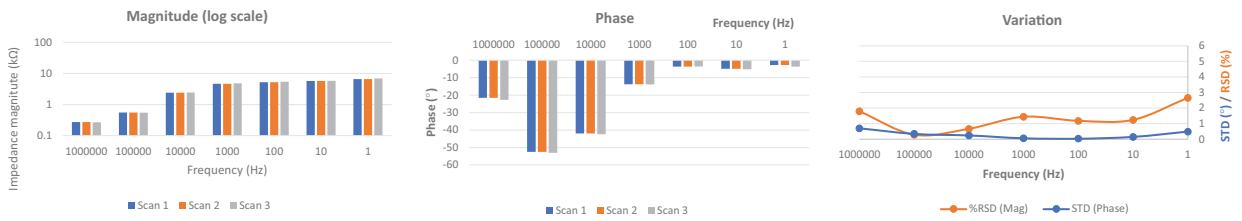
**Location 1 (3D printed probe)**



**Location 2 (3D printed probe)**



**Location 3 (3D printed probe)**



**Location 1 (Concentric ring probe)**



**Location 2 (Concentric ring probe)**

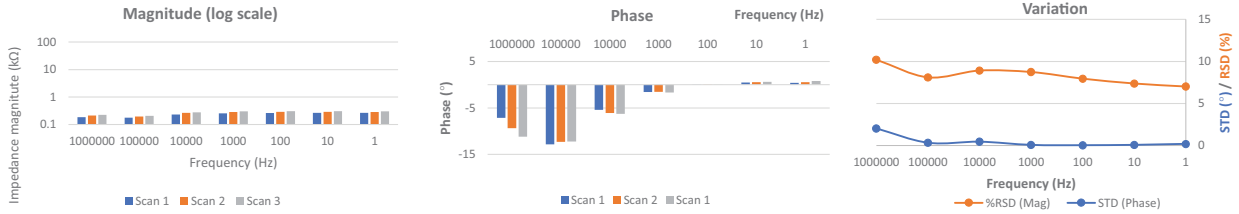


**Location 3 (Concentric ring probe)**

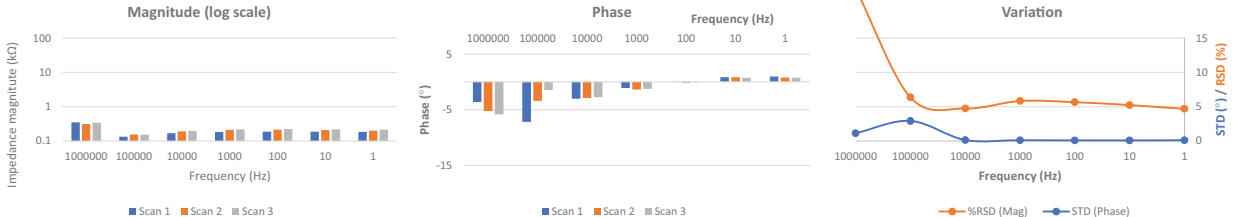


**Figure 7.** Impedance magnitude (left panel) and phase (middle panel) values at seven discrete frequencies (1 Hz to 1 MHz) in repeated BIS measurements (three scans) for cucumber sample. Inter-scan variation graphs (right panel) show relative standard deviation (RSD, %) of impedance magnitude and standard deviation (STD, °) of phase data. Data obtained with the 3D printed probe (upper part of figure) are shown in comparison to the concentric ring probe data (lower part of figure).

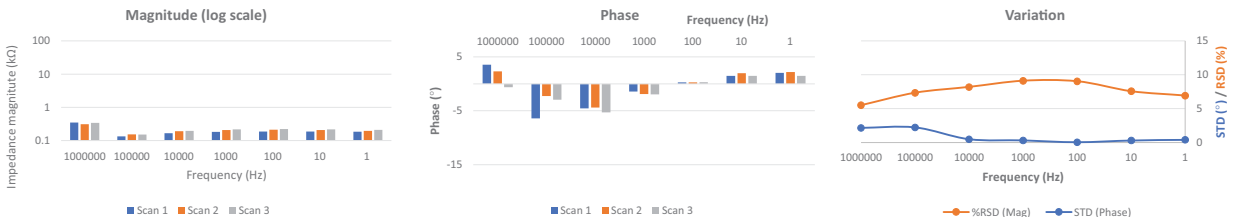
**Location 1 (3D printed probe)**



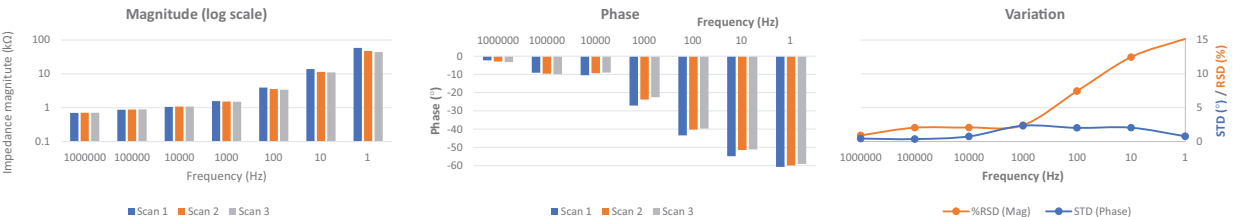
**Location 2 (3D printed probe)**



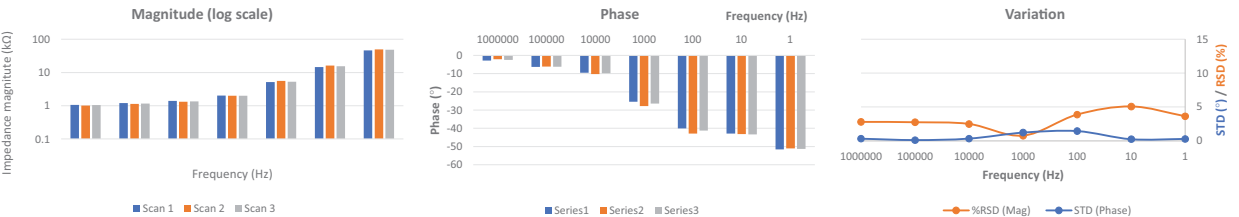
**Location 3 (3D printed probe)**



**Location 1 (Concentric ring probe)**



**Location 2 (Concentric ring probe)**



**Location 3 (Concentric ring probe)**



**Figure 8.** Impedance magnitude (left panel) and phase (middle panel) values at seven discrete frequencies (1 Hz to 1 MHz) in repeated BIS measurements (three scans) for porcine tongue sample. Inter-scan variation graphs (right panel) show relative standard deviation (RSD, %) of impedance magnitude and standard deviation (STD, °) of phase data. Data obtained with the 3D printed probe (upper part of figure) is shown in comparison to the concentric ring probe data (lower part of figure).



for sensitive BIS measurements. On the other hand, 3D printed material used in probe head (plastic holder) plays also an important role in this type of probe in terms of providing adequate electrical insulation between the electrodes in wet measurement conditions. Most of the 3D printed plastic holders were constructed using a single 3D printable material (Formlabs Standard Clear FLGPCL04). However, two other materials, i.e., printable multi-material (Vero PureWhite) and Teflon sheets (used in handmade probe) were also used but those were not optimal for this kind of BIS measurements. Finally, we got the success with high purity silver (Ag) plate electrodes inserted inside the 3D printed plastic made frame using single material insulation. In the future, it is worth testing the possibility of preparing all the probe components including electrodes, frame and connectors by 3D printing as soon as the metallic electrode materials such as high purity silver become available. High accuracy of printing process allows good mechanical contact in electrical contacts without soldering. Other advantages of 3D printing include flexibility in controlling size and geometry and possibilities for curved or flexible designs. Moreover, such 3D printed probe is possible to adjust with ideal surface roughness and porosity. Further investigations are also needed to clarify the usefulness of Ag/AgCl coatings on four-terminal probes. Electrodeposited AgCl is known to provide low contact impedance and interfacial properties that approach the characteristics of a perfectly non-polarisable electrodes [21]. However, there are also some shortcomings related to weak durability of these coatings. Furthermore, the importance of low contact impedance is not so emphasised in four-terminal measurement.

The present 3D printed probe with four Ag electrodes, intended to be used for assessing oral mucosal health via BIS measurements, showed excellent linearity ( $R^2=0.999$ ) in diluted saline solution measurement over a wide conductivity range (0.25–8 mS/cm). This conductivity range covers well the range of values for the different biological tissues [22]. Figure 6 shows that the impedance phase of NaCl solutions is very close to zero, as it should be for these kinds of electrolytic solutions, and therefore any measured phase deflecting from zero can be considered as an error or artefact. According to Emran et al. [9] and Balmer et al. [23], a parasitic capacitance (i.e., stray capacitance) is an important factor for the sharp decrease in the impedance modulus and rise in the phase. Our probe and the leads between the probe and the Solartron analyser also showed the similar issue and

thus we limited the visualisation of spectral images (see Figure 6) and analyses for the frequencies below 1 MHz.

We compared the data obtained with the 3D printed probe on cucumber and porcine tongue samples to that measured with the previously introduced concentric ring probe [9]. There are some clear spectral differences between the probe types (Figures 7 and 8). With the 3D printed probe impedance magnitudes were generally lower and highly independent on excitation frequency whereas with the concentric probe they were much higher and frequency dependent. This was as expected because the four-terminal method used in the 3D printed probe employs separate electrode pairs for current injection and voltage measurement and it thus eliminates the contact impedance from the measurement. Naturally, the material selection also plays a role, but only in a minor extent because the current carrying properties over metal/electrolyte interfaces are demonstrated to be similar in silver and SS electrodes [24,25]. Therefore, four-electrode method will increase the measurement stability and lower inter-scan variability. We found that the RSDs of impedance magnitude for cucumber sample were below 3.5% when 3D printed probe was used whereas in the concentric ring probe measurements the corresponding varied more between the different locations and the highest RSDs were close to 6%. Similarly, RSDs of impedance magnitude varied less between the repeated porcine tongue sample measurements when the concentric ring probe was used. A good reproducibility of the measurement is very important issue when attempting to detect small differences in the electrical properties of biological tissues and one important merit in the present 3D printed probe.

Our study with the concentric ring probe showed that there is a trend towards slightly decreased impedance magnitudes from the first scan to the third one. Interestingly, this trend was missing when 3D printed probe was used. Instead, there was a trend towards slightly increased impedance magnitudes from the first scan to the third one. One explanation for that is that in two terminal measurements (concentric ring probe) electrode-tissue contact improves over time that lowers the impedance. Since four-terminal (3D printed probe) measurement is not influenced by contact impedance, observed phenomena was opposite in its direction. This slight increase in impedance magnitude was most likely related to sample drying and viscoelastic properties of biological samples [26]. We used the same weight 200 g (0.03 MPa) for both

configurations that was optimised in our previous study to provide most consistent results [9]. However, further studies are needed to clarify the importance of fixed pressure when the tetrapolar 3D printed probe is used. For taking next steps towards clinical (*in vivo*) application, we will also study how consistent results can be achieved if measurements are performed by hand-held probe with contact pressure control instead of placing it in the stand. This could be realised by using force indicator or proper spring loading at least at the probe tip. Furthermore, in the future, it is worth testing the possibility of preparing all the probe components including electrodes, frame and connectors by 3D printing as soon as the metallic electrode materials such as high purity silver becomes available.

## 5. Conclusions

In order to prevent malignant transformation of oral premalignant lesions, new non-invasive point-of-care detection techniques are needed. Bioimpedance spectroscopy could be a viable method to assess pathological changes in oral mucosal tissues. However, hand-made probes often suffer from low manufacturing and measurement reproducibility. This study demonstrated that 3D printing technique is feasible method to construct highly accurate and reproducible BIS probes. The present tetrapolar 3D printed probe can reliably characterise the biological samples having different electrical conductivity properties. In the future, it is worth testing the possibility of preparing all the probe components including electrodes, frame and connectors by 3D printing, and to clarify the importance of fixed pressure especially when the probe is used as a hand-held apparatus.

## Acknowledgements

The authors acknowledge Savonia University of Applied Sciences and M.Sc. Noora Toropainen for their help with 3D printing.

## Disclosure statement

No potential conflict of interest was reported by the author(s).

## Funding

This research was partly funded by the Regional Council of Pohjois-Savo (3DPMED project), the Finnish Cultural Foundation and the Foundation of Päivikki and Sakari Sohlberg.

## ORCID

Shekh Emran  <http://orcid.org/0000-0003-1897-3268>

Sami Myllymaa  <http://orcid.org/0000-0002-9779-4358>

## References

- [1] Ferlay J, Soerjomataram I, Dikshit R, et al. Cancer incidence and mortality worldwide: sources, methods and major patterns in GLOBOCAN 2012. *Int J Cancer*. 2015;136(5):E359–E386.
- [2] Baykul T, Yilmaz H, Aydin Ü, et al. Early diagnosis of oral cancer. *J Int Med Res*. 2010;38(3):737–749.
- [3] Emran S, Hurskainen M, Tomppo L, et al. Bioimpedance spectroscopy and spectral camera techniques in detection of oral mucosal diseases: a narrative review of the state-of-the-art. *J Med Eng Technol*. 2019;43(8):474–491.
- [4] Cawson RA, Odell EW, Porter SR. *Cawson's essentials of oral pathology and oral medicine*. 7th ed. New York: Churchill Livingstone; 2002. p. 243–254.
- [5] Steele TO, Meyers A. Early detection of premalignant lesions and oral cancer. *Otolaryngol Clin North Am*. 2011;44(1):221–229.
- [6] Warnakulasuriya S, Johnson NW, van der Waal I. Nomenclature and classification of potentially malignant disorders of the oral mucosa. *J Oral Pathol Med*. 2007;36(10):575–580.
- [7] Messadi DV. Diagnostic aids for detection of oral precancerous conditions. *Int J Oral Sci*. 2013;5(2):59–65.
- [8] Nair DR, Pruthy R, Pawar U, et al. Oral cancer: premalignant conditions and screening—an update. *J Cancer Res Ther*. 2012;8(Suppl. 1):S57–S66.
- [9] Emran S, Lappalainen R, Kullaa AM, et al. Concentric ring probe for bioimpedance spectroscopic measurements: design and ex vivo feasibility testing on pork oral tissues. *Sensors (Basel, Switzerland)*. 2018;18(10):3378.
- [10] Anonymous design of bioimpedance spectroscopy instrument with compensation techniques for soft tissue characterization. *J Med Devices*. 2015;9:210011.
- [11] D'Orazio AI, Fisher MD, O'Shaughnessy J. Highlights from: 24th Annual San Antonio Breast Cancer Symposium, San Antonio, Texas, December 10–13, 2001. *Clin Breast Cancer*. 2001;2:260–265.
- [12] Malvey J, Hauschild A, Curiel-Lewandrowski C, et al. Clinical performance of the Nevisense system in cutaneous melanoma detection: an international, multicentre, prospective and blinded clinical trial on efficacy and safety. *Br J Dermatol*. 2014;171(5):1099–1107.
- [13] Braun RP, Mangana J, Goldinger S, et al. Electrical impedance spectroscopy in skin cancer diagnosis. *Dermatol Clin*. 2017;35(4):489–493.
- [14] Aberg P, Nicander I, Hansson J, et al. Skin cancer identification using multifrequency electrical impedance—a potential screening tool. *IEEE Trans Biomed Eng*. 2004;51(12):2097–2102.
- [15] Mohr P, Birgersson U, Berking C, et al. Electrical impedance spectroscopy as a potential adjunct diagnostic tool for cutaneous melanoma. *Skin Res Technol*. 2013;19(2):75–83.

- [16] Murdoch C, Brown BH, Hearnden V, et al. Use of electrical impedance spectroscopy to detect malignant and potentially malignant oral lesions. *Int J Nanomedicine*. 2014;9:4521–4532.
- [17] Richter I, Alajbeg I, Boras VV, et al. Mapping electrical impedance spectra of the healthy oral mucosa: a pilot study. *Acta Stomatol Croat*. 2015;49(4):331–339.
- [18] Grossi M, Riccò B. Electrical impedance spectroscopy (EIS) for biological analysis and food characterization: a review. *J Sens Sens Syst*. 2017;6(2):303–325.
- [19] Yufera A, Rueda A. A method for bioimpedance measure with four- and two-electrode sensor systems. *Annu Int Conf IEEE Eng Med Biol Soc*. 2008;2008:2318–2321.
- [20] Robin A. Corrosion behavior of niobium, tantalum and their alloys in boiling sulfuric acid solutions. *Int J Refract Met Hard Mater*. 1997;15(5–6):317–323.
- [21] Myllymaa S, Pirinen S, Myllymaa K, et al. Improving electrochemical performance of flexible thin film electrodes with micropillar array structures. *Meas Sci Technol*. 2012;23(12):125701.
- [22] Peters MJ, Stinstra JG, Leveles L, et al. The electrical conductivity of living tissue: a parameter in the bioelectrical inverse problem. In: He B, editor. *Modeling and imaging of bioelectrical activity*. Boston (MA): Springer; 2004. p. 281–319.
- [23] Balmer TW, Vesztergom S, Broekmann P, et al. Characterization of the electrical conductivity of bone and its correlation to osseous structure. *Sci Rep*. 2018; 8(1):8601–8608.
- [24] Ragheb T, Geddes LA. Electrical properties of metallic electrodes. *Med Biol Eng Comput*. 1990;28(2): 182–186.
- [25] Mirtaheri P, Grimnes S, Martinsen G. Electrode polarization impedance in weak NaCl aqueous solutions. *IEEE Trans Biomed Eng*. 2005;52(12):2093–2099.
- [26] Glahder J, Norrild B, Persson MB, et al. Transfection of HeLa-cells with pEGFP plasmid by impedance power-assisted electroporation. *Biotechnol Bioeng*. 2005; 92(3):267–276.